Special Contributions, Geophysical Institute, Kyoto University, No. 4, 1964, 37-49

STUDY OF FOCAL MECHANISM BY THE ANALYSIS OF SEISMIC WAVES OF S-TYPE

By

Michio OTSUKA

(Received October 15, 1964)

Abstract

An attempt was made to interpret variations in the waveforms of S and ScS phases from a deep-focus earthquake as due to the azimuthal difference in patterns of wave emission at the origin. A comparison of the recorded waveforms with the corresponding theoretical seismograms shows a possibility that the waveforms of both phases could be explained by the superposition of simple wavelets emitted from progressing faults. The fault plane determined from the analysis of the waveforms of S and ScS was consistent with that from the usual method based on P wave data.

Introduction

Author pointed out in the previous paper (Otsuka, [1962]) that the waveforms of ScS phases in some deep-focus earthquakes are very simple, while those of S phases in the pertaining earthquakes are more or less complicated. Subsequent investigations, however, have shown that this rule does not always hold, but seismic waveforms exhibit more extravagant appearances even when our scopes are restricted to such phases as sS, SS, ScS, SSS etc., which were all emitted out from foci originally as shear waves.

In the following articles, an attempt will be made to interpret variations in the waveforms of S and ScS phases from a deep-focus earthquake as due to the azimuthal difference in patterns of wave emission at a seismic focus.

Method of analysis

In discussing the waveforms of seismic waves, the most effective factor to be taken into consideration is the superposition of other disturbances. Discussions on the waveforms of near earthquakes encounter a great deal of difficulties originated from this effect. In seismograms of deep and/or distant earthquakes, however, it is often the case that each phase is separated enough and clearly identified.

A method of analysis proposed here is applicable only to such simple wavelets.

In calculating the true ground motion from a seismogram, it is necessary in the first place to remove the effects of seismograph. In principle, it can be achieved

by integrating the recorded deflections on seismogram through the equations of motion of seismograph. This method, however, is troublesome and inaccurate, because the result of calculation is very sensitive to the errors in position or tilting of zero line of the seismogram.

The method of comparing the actual seismograms with the calculated responses of seismograph against variously assumed ground motions will be adopted as an alternative in the following discussions. This method is not applicable to investigate the minute structure of ground motion, but it may be effective for the purpose of scanning many seismograms, especially when the rough features of ground motion are known beforehand.

Proposed model of seismic origin

When a certain seismic phase is separated enough in time from other disturbances and clearly identified in seismograms, let us call it wavelet, after N. Ricker [1953].

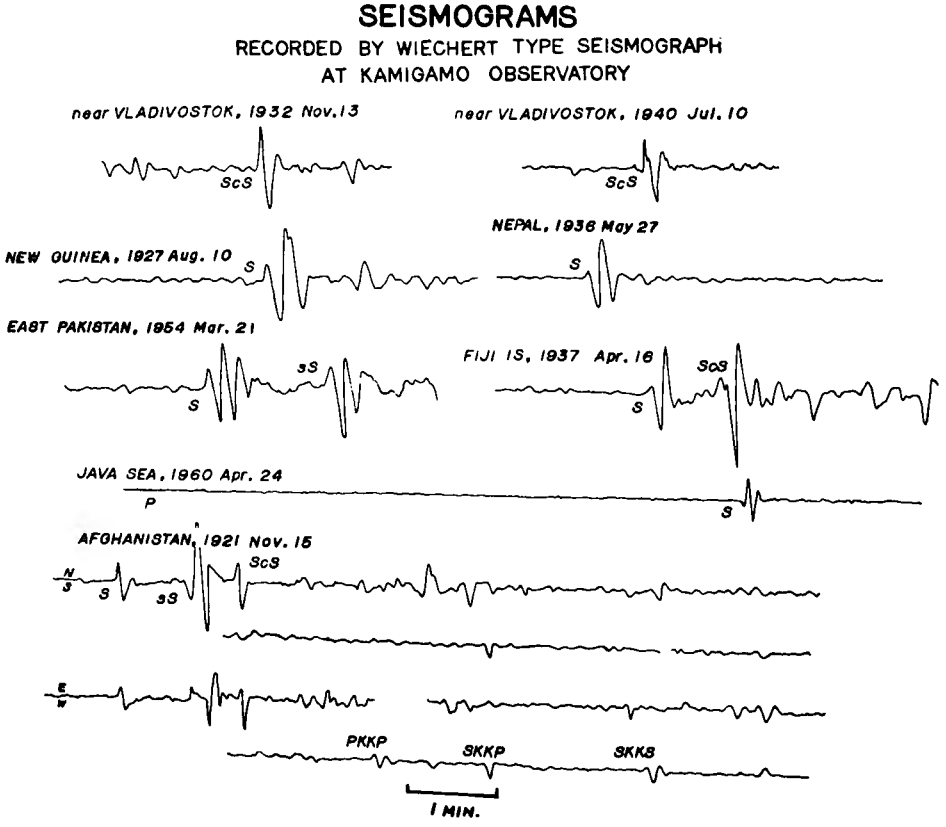

Fig. 1. Examples of wavelets observed by the Wiechert-type seismograph at the Kamigamo Observatory.

In Fig. 1 are shown a few of the examples of wavelets obtained by the Wiechert-type seismograph with a natural period of 10 sec. at the Kamigamo Observatory in Kyoto. Since clear wavelets were found only in seismic phases of shear type, the following discussions are to be understood as to concern exclusively with this type of wavelets. Looking into the forms of the wavelets, it is understood that, in some cases, each of them bears a striking resemblance despite that they belong to different earthquakes, but in others, various phases are quite different in the waveform even when they belong to the same earthquake.

This fact seems to suggest that the mechanism of seismic wave generation at the source is more effective on the characterization of the waveform than the path of wave transmission, as long as shear phases of deep or distant earthquakes are concerned; there is a possibility that the waveforms of seismic wavelets could be explained by a certain mechanism of seismic wave generation common to all earthquakes.

Fig. 2 is a schematical representation of the proposed model of a seismic focus. Let us assume that a fracture of material originates from a point P and proceeds along a straight line to another point Q, incessantly emitting out elastic waves. As a result, an observer will observe the resultant of every motion caused by the waves from each line-segment between P and Q.

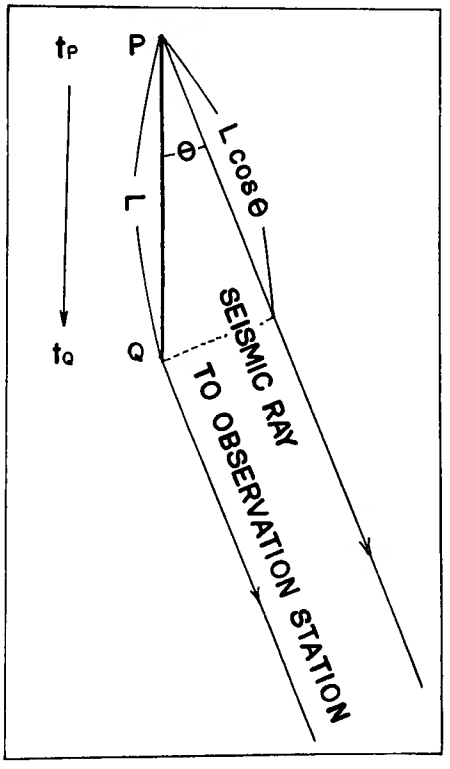

Fig. 2. Proposed model of seismic origin.

Now, let us designate the time of occurrence of fracture at P as t_P, and the time of termination of fracture at Q as t_Q. If L is the length of a line PQ and V_f is the velocity of fracture progression from P to Q, the time needed for formation of the whole fracture is expressed as follows:

$$t_Q - t_P = \frac{L}{V_f}. \qquad (1)$$

An observation station which is located toward a direction of θ measured from the

direction PQ, and considerably distant from P, will observe the wave fronts from P and Q at

$$t_1 = t_P + \frac{D}{V_S} \quad \text{and} \quad t_2 = t_Q + \frac{D - L\cos\theta}{V_S}, \tag{2}$$

respectively, where D denotes the distance from P to the observation station measured along the path of wave transmission, and V_S denotes the velocity of propagation of shear waves in the medium. If V_f is smaller than V_P, the apparent duration-time (time difference in arrivals of pulses from P and from Q) at the observation station is $t_2 - t_1$ ($\equiv t^*$) Taking eqs. (1) and (2) into consideration, the following expression is obtained for t^*:

$$t^* = \left(\frac{1}{V_f} - \frac{1}{V_S}\cos\theta\right)L. \tag{3}$$

Since it was assumed that elastic waves are incessantly emitted out as the fracture proceeds from P to Q, they reach the observation station during the period of t^*. This mechanism of fault progression has been suggested by Benioff [1955] for explaining an azimuthal effect on wavelet emission. Fig. 3 taken from his paper shows the

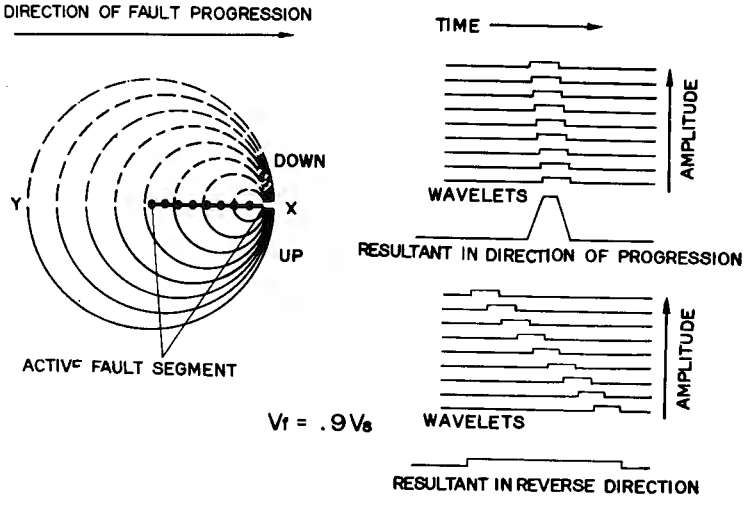

Fig. 3. Mechanism for azimuthal effect on wavelet emission by fault progression, after Benioff [1955].

mechanism in a schematical way. If V_f is slightly less than V_S the azimuthal effect on t^* becomes very conspicuous. If V_f/V_S is 0.9, as Benioff assumed, the azimuthal dependence of t^* is expressed as

$$t^* = \frac{L}{V_S}(1.11 - \cos\theta). \tag{4}$$

When θ is small, the apparent duration-time is short. The larger θ becomes, the longer t^* grows. The apparent duration-time in the reverse direction to fracture progression is as about 19 times long as that in the direction of fracture progression. It is of natural consequence that waveforms of seismic wavelets depend on the azimuth of observation station seen from the direction of fracture progression.

Calculation of the waveforms of seismic wavelets

Calculation of the waveforms of seismic wavelets to be recorded at an observation station is performed by summing up contributions of waves to seismographs from every small line-segments between P and Q.

If the waveforms of seismic wavelets from a unit length of line segments between P and Q are assumed to be always the same, (hereafter referred to as a unit wavelet and denoted by $f(t)$), and its intensity, to be kept constant throughout the formation of fracture PQ, the ground motion to be recorded at an observation station, in case of neglecting the effects of path of wave transmission and of ground surface, would be of the form:

$$\int_0^L f\left(t-\frac{x}{V_f}+\frac{D-x\cos\theta}{V_S}\right)dx\,. \quad (5)$$

Responses of a seismograph against the ground motion expressed by eq. (5) are to be calculated if we know the functional form of unit wavelet $f(t)$ and constants of the seismograph.

The author has shown in the previous paper that the simplest pattern often found in seismograms of ScS phases suggests that the ground motion is of very simple pattern having a single peak and smooth skirts on both sides. This aspect was also supported by the investigation of deep-focus earthquakes by Kasahara [1963].

Fig. 4 shows some examples of the collation for a few types of one-sided simple

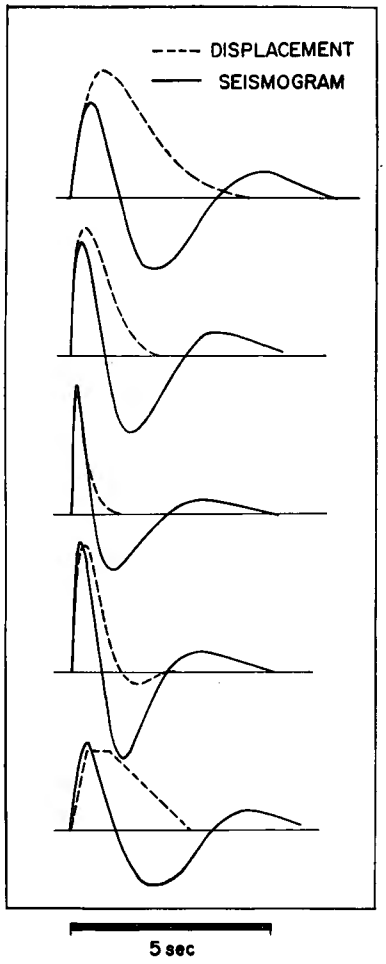

Fig. 4. Assumed ground motions and corresponding wavelets to be recorded by the Wiechert-type seismograph.

ground motion and the corresponding responses of the Wiechert-type seismograph, the free period and damping constant of which were assumed to be 5.0 sec. and 0.5, respectively, and its solid friction was neglected. It is remarkable that the ScS phases in the uppermost traces in Fig. 1 are very similar to these simple patterns of ground motion. It is also to be noted that slight modifications in the waveform of the assumed ground motions give no serious effects on the shape of the theoretical seismograms.

Here, we introduce a hypothesis that the unit wavelet is of Berlage's type:

$$f(t) = A t e^{-\gamma t} \sin \omega_0 t \,, \qquad (6)$$

where

$\omega_0 = 2\pi/\tau$,

τ = the period of unit wavelet ,

A = an arbitrary constant ,

and

$\gamma = \omega_0$.

Some examples of the theoretical seismograms to be recorded by a seismograph of Wiechert-type located at a station toward the direction of θ from PQ are shown in Fig. 5. L, V_S and V_f/V_S were assumed to be 20 km, 5.0 km/sec. and 0.9, respectively in these examples. Calculation was made for θ of 0, 30, ..., 180 degrees and τ of 1.25, 2.5, 5.0, and 10.0 sec. respectively. It may be noticed that while wavelets in the direction of fracture progression are similar in shape to those in Fig. 4, the composite

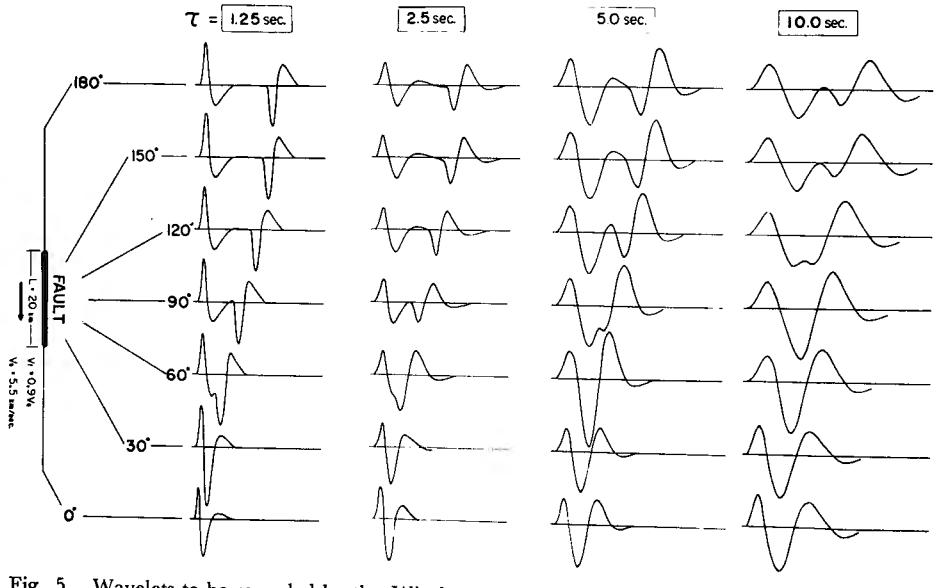

Fig. 5. Wavelets to be recorded by the Wiechert-type seismograph located toward a direction θ.

waveforms are gradually distorted as θ increases until a separation into two wavelets occurs. It is interesting to note that various patterns in the calculated seismograms, as shown in Fig. 4, can often be found as wavelets in actual seismograms.

Although calculations of the wavelets in Fig. 5 were made under the assumption that $f(t)$ is expressed by eq. (6), alterations of the functional form of $f(t)$ may not cause serious effects on the above described characteristics of calculated wavelets.

If we find out adequate correspondences between the actual and calculated seismograms of a certain earthquake, we may be allowed as a next step to deduce a geometrical relation between the fracture and emitted seismic rays.

Determination of the direction of fracture progression

Direction of fracture progression may be determined in the following way.

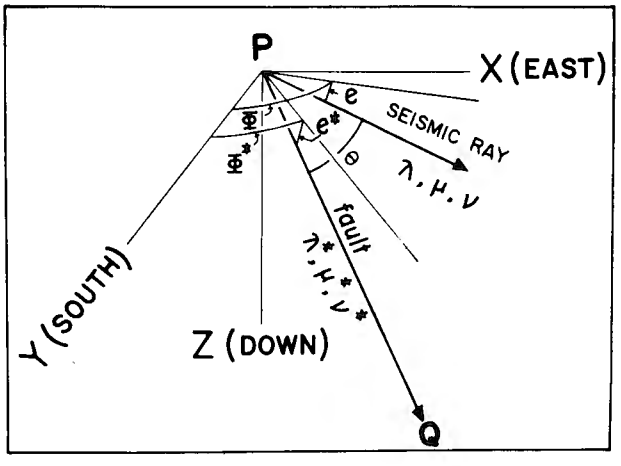

Fig. 6. Co-ordinates at the seismic focus.

Take the starting point P of a fracture as the origin of the Cartesian co-ordinate and the x-, y- and z-axes, east-, south- and down-wards, respectively, as shown in Fig. 6. Let the direction cosines of a fracture direction PQ be λ^*, μ^* and ν^*, and the direction cosines of a seismic ray starting from P and extending to the observation station in question be λ, μ and ν. If the emergent angle of the seismic ray at P is denoted by e, and the azimuth of the observation station as seen from P measured from the y-axis is denoted by Φ, the following relations exist:

$$\lambda = \cos e \sin \Phi ,$$

$$\mu = \cos e \cos \Phi ,$$

and

$$\nu = \sin e . \qquad (7)$$

Fig. 7 shows the geometrical relationships of epicenter E, observation station O and the north pole P on the earth's surface. Φ is related to the longitude of the observation station λ_0, longitude of the epicenter λ_E, latitude of the observation station φ_0 and epicentral distance Δ by the following expression:

$$\sin \Phi = \frac{\sin (\lambda_0 - \lambda_E)}{\sin \Delta} \cos \varphi_0 . \quad (8)$$

The emergent angle e can be calculated by the relation:

$$\sin (90° - e) = \frac{V_S}{r} \left(\frac{dT}{d\Delta} \right), \quad (9)$$

where V_S is the velocity of S waves in the neighbourhood of focus, r is the distance between P and the earth's center and $dT/d\Delta$ is the gradient of a travel time curve of the seismic ray in question. The direction cosines λ, μ, ν, λ^*, μ^* and ν^* satisfy the expressions:

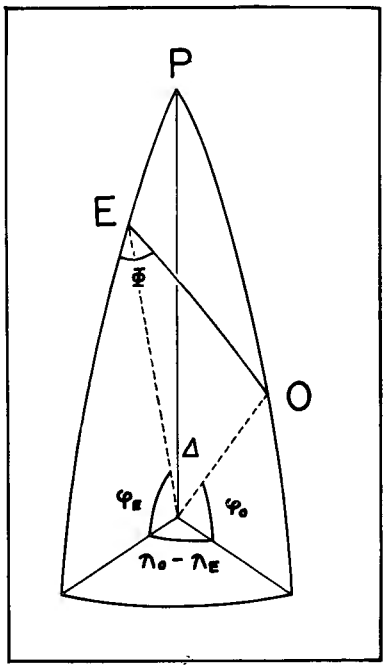

Fig. 7. Geometrical relationship of epicenter and observation station on the earth's surface.

$$\lambda\lambda^* + \mu\mu^* + \nu\nu^* = \cos \theta \quad (10)$$

and

$$\lambda^{*2} + \mu^{*2} + \nu^{*2} = 1 . \quad (11)$$

In eqs. (10) and (11), λ^*, μ^* and ν^* are to be determined. If θ's are determined, therefore, by using the foregoing technique of comparing wavelets for two stations, λ^*, μ^* and ν^* can be obtained by solving three simultaneous equations. As eq. (11) is quadratic, two sets of solution are generally obtained, of which reasonable one is to be selected if another informations are available.

Deep-focus earthquakes of Jan. 3, 1957

Now, let us apply the above procedure to a deep-focus earthquake. The time of occurrence, location of epicenter etc. are as follows:

Time of occurrence : 1957 Jan. 3^{rd}, 12^h 48^m 03.5^s (GMT)
Location of epicenter: 43 $\frac{1}{2}$°N, 131 $\frac{1}{2}$°E
Depth of hypocenter : 600 km
Magnitude : 7

S and ScS phases of this earthquake are very clearly identified in the seismograms obtained in Japan.

Among many seismograms, S and ScS phases, which have been observed by the Wiechert-type seismographs of a free period of 5 sec. equipped at Morioka ($\lambda = 141°$ 10.2′E, $\varphi = 39°$ 41.7′N) and Shimizu ($\lambda = 132°57.7'$E, $\varphi = 32°46.5'$N), were selected and compared with the calculated wavelets. Fig. 8 shows the collations of the actual and calculated wavelets. The theoretical wavelets were calculated under the assumption that L, V_S and V_f/V_S are 20 km, 5 km/sec. and 0.9, respectively. Among

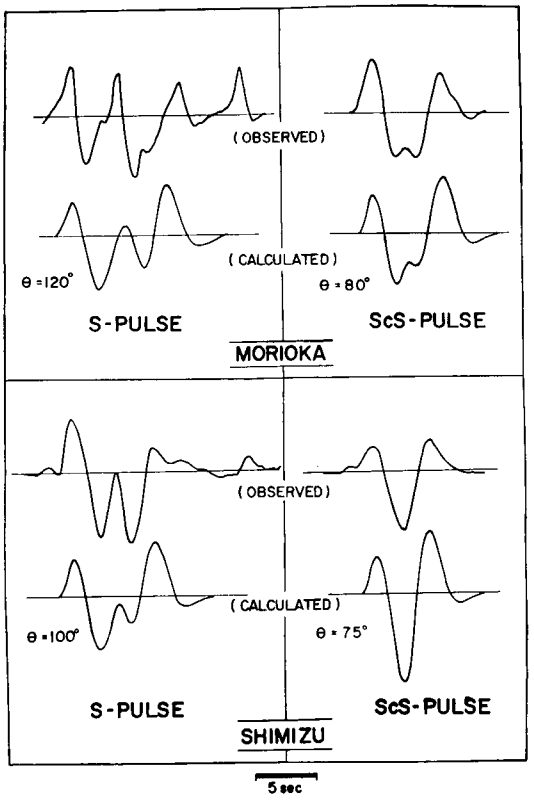

Fig. 8. Collations of the actual and calculated wavelets.

various numerical values that were tried, this combination has been proved to give the most satisfactory result, in view of the analysis of the initial motions of P waves as shown in the following.

If eq. (10) and eq. (11) are solved for θ's of ScS of Morioka and that of Shimizu, the solution gives a direction of fracture progression of

azimuth of S 62°W and dip of 13° downward (a)

or

azimuth of S 1°W and dip of 10° downward. (b)

Neither of these solutions suffice θ's of S of Morioka and Shimizu. On the other hand, if eq. (10) and eq. (11) are solved for θ's of S for Morioka and Shimizu, the solution gives another direction of fracture progression of

azimuth of N 66°W and dip of 3° upward (c)

or

azimuth of N 42°W and dip of 51° downward. (d)

Again, neither of these solutions suffice θ's of ScS of Morioka and Shimizu.

This discrepancy might be due to inadequate assumptions made for the length of fracture, rupture velocity etc., but the model of one-dimensional fracture progression should also be reappraised. Two-dimensional growth of fracture in the medium seems to be rather plausible. In that case, the preceding discussions should be modified.

Let us assume that the fracture originated from a point P develops two-dimensionally to form a fan-shaped fault plane PQ_1Q_2, as shown schematically in Fig. 9.

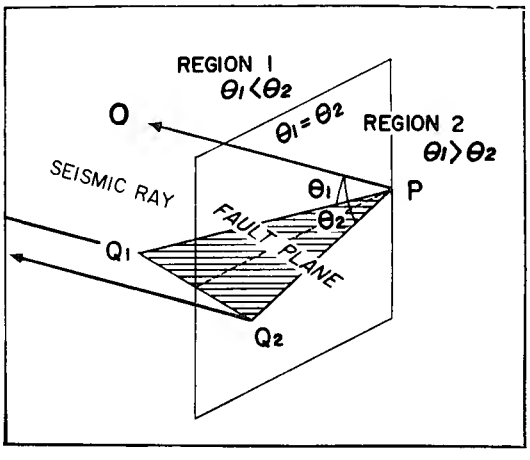

Fig. 9. Seismic ray and fault plane.

Wavelets to be observed at any observation station are a resultant of contributions of unit wavelets from each small segment of the fault plane PQ_1Q_2. An accumulation of the contributions of unit wavelets may cause various displacement patterns depending on the location of observation station relative to the fault plane PQ_1Q_2. If the fracture velocity is smaller than the elastic wave velocity in the vicinity of focus, the initial wave pulses come from P at all observation stations, but the final pulses may come from Q_1 or Q_2, depending on which region a seismic ray OP belongs to. If OP lies in the region in which $\angle OPQ_1\ (=\theta_1) < \angle OPQ_2\ (=\theta_2)$ (region 1), the apparent duration-time of the observed wavelet may be governed by θ_2, and vice

versa. In other words, it may be governed by the larger of θ_1 and θ_2. If intensity variations due to the accumulation of contributions from each segment of the fault plane are disregarded, the waveforms of seismic wavelets are determined by a single parameter θ_1 or θ_2, and the same discussion as in the case of one-dimensional fracture progression is available.

If the directions of fracture progression (a) or (b) and (c) or (d) determined in the preceding studies are assumed to correspond to PQ_1 and PQ_2, four fault planes are defined by combinations of pairs of the fracture directions.

It is known both in theory and from the analysis of distribution of initial motions of seismic waves that one of the nodal planes coincides with the fault plane around an origin sphere. So, if a pair of fracture directions define a fault plane, it must be in harmony with informations from the distribution of initial motions of P waves.

The distribution of the initial motion of P waves in this earthquake is kataseismic at most of the observation stations in Japan except for Saga in northern Kyushu, which observed a small anaseismic initial motion. Large amplitudes of the initial motions are observed in central Honshu, and decrease gradually west- and north-ward as shown by arrows in Fig. 10, suggesting the existence of a nodal line at the western part

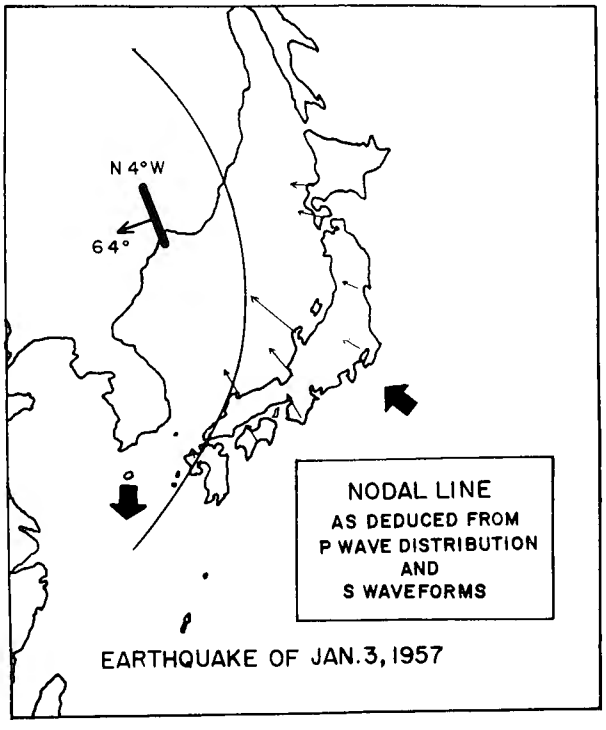

Fig. 10. Nodal line of the deep-focus earthquake of Jan. 3, 1957, deduced from P wave distribution and waveforms of S wavelets.

of Kyushu.

Examining every four pairs of fracture directions, the combination of (b) and (d) proved to give the most satisfactory agreement with the P wave data.

Fault, thus defined, is a fan-shaped plane of a strike of N 4°W, dipping 64° westward, and the nodal line expected from the fault is as shown in Fig. 10. It seems to be quite reasonable, so long as the distribution of initial P motions are concerned.

Deep-focus earthquake of Sept. 28, 1957

Fig. 11 shows the location of epicenter of the deep-focus earthquake of Sept. 28, 1957, locations of five chosen stations, and the S-wavelets observed by the Wiechert-type seismographs at each of the pertaining stations. It is noted that the waveforms of these wavelets quite correspond also to what we have treated in the preceding sections. A remarkable fact is that the wave breadths are maximum for Sumoto, and contracts both north- and west-ward, suggesting the relevance of the moving source hypothesis.

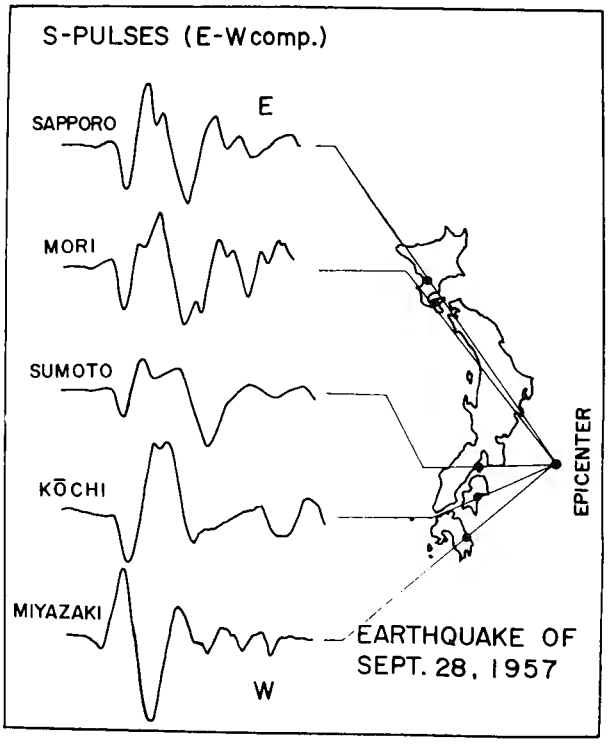

Fig. 11. Location of epicenter of the deep-focus earthquake of Sept. 28, 1957, location of five chosen stations and S wavelets observed at each pertaining station.

It is impossible, however, to relate the waveforms to the mechanism of seismic origin, because other phases are not available in the seismograms of this earthquake.

Concluding remarks

S-type wavelets in two deep-focus earthquakes were presumed to be related to the mechanism of seismic origin. The fault plane as deduced from waveforms of either of S and ScS phases could be so determined as to be in harmony with P wave data.

Waveforms of S-type wavelets observed with mechanical seismographs, however, do not always correspond to any one of the wavelets in Fig. 5, but various patterns are met in actual seismograms. That, of course, will demand alterations of the assumptions made in our discussions such as on the functional form of $f(t)$, intensity of contributions from each segment of fault plane etc.

More detailed examinations of these assumptions are to be made in another publication.

Acknowledgements

The present author wishes to express his deepest grief to the late Professor Eiichi Nishimura's sudden death as well as sincere gratitude for his encouragement throughout the present study. His thanks also go to Dr. Takeshi Mikumo for his helpful suggestions and discussions. The author is much indebted to the directors and members of the Central and Provincial Meteorological Observatories in Japan for their kind permission for copying seismograms obtained at their observatories.

References

Benioff, H., 1955; Earthquakes in Kern County during 1952, Calif. Dept. Nat. Resources. Div. Mines, Bull., 171, 199-202.

Kasahara, K., 1963; Waveform analysis of S-pulses from deep-focus earthquakes. Part I, Bull. Earthq. Res. Inst., 41, 209-216.

Otsuka, M., 1962; On the forms of S and ScS waves of some deep earthquakes, J. Seism. Soc. Japan, Ser. 2, 15, 169-182.

Ricker, N., 1953; The form and laws of propagation of seismic wavelets, Geophysics, 18, 10-40.